

## Key intermediates in the synthesis of enantiopure antagonists at NMDA receptors: a structural study

Gabriella Bombieri,\* Nicoletta Marchini, Fiorella Meneghetti,  
Andrea Pinto and Gabriella Roda

*Istituto di Chimica Farmaceutica e Tossicologica, Università di Milano, Viale Abruzzi 42, I-20131 Milano, Italy*

Received 28 June 2005; accepted 28 July 2005

**Abstract**—The two diastereomeric amino acid derivatives **8** (3*aS*,5*R*,6*aS*)-5-*tert*-butoxycarbonylamino-4,5,6,6*a*-tetrahydro-3*aH*-cyclopenta[*d*]isoxazole-3,5-dicarboxylic acid diethyl ester, its epimer **9** (3*aS*,5*S*,6*aS*), and carboxylic acid **10** obtained by hydrolysis of **9**, which are intermediates in the synthesis of novel NMDA receptor antagonists **6** and **7** (Fig. 1), have been characterized by X-ray studies at 293 K for **8** and **10**, and at 100 K for **9**. The configuration of the carbon binding the 5-*tert*-butoxycarbonylamino moiety (BOC) determines the different molecular complexity: the chain structure for **8**, dimeric for **9**, and chain dimers for **10**. The pharmacophoric parameters in compound **8** (from which the active **7** is derived) are comparable with those observed for NMDA receptor antagonism, while **9** and **10** do not present the structural features, which match these pharmacophoric characteristics. © 2005 Elsevier Ltd. All rights reserved.

### 1. Introduction

(*S*)-Glutamic acid **1** (Glu) (Fig. 1) is the main excitatory neurotransmitter in the central nervous system, where it is involved in the physiological regulation of processes such as learning and memory.<sup>1–3</sup> Its glutamatergic hyperactivity leads to neurotoxicity typical of some acute and chronic neurodegenerative diseases.<sup>1–3</sup>

Two families, the ionotropic receptors (iGluRs) and the metabotropic receptors (mGluRs),<sup>1–6</sup> are the specific receptors for Glu. The modulation of the glutamatergic pathways represents a relevant therapeutic approach in the treatment of a number of neurodegenerative pathologies, neuropsychiatric diseases, as well as learning and memory impairments. Experimental evidence suggests the potential therapeutic application of *N*-methyl-D-aspartic acid (NMDA) antagonists in the treatment of cerebral ischemia and other neurodegenerative disorders.<sup>7,8</sup> So far, a large number of competitive and non-competitive NMDA antagonists have been tested as drug candidates. Unfortunately, almost all of them have shown unacceptable adverse effects in humans, that is, psychotomimetic and cardiovascular side effects.<sup>9</sup>

Recently, the approval of a non-competitive NMDA antagonist for the treatment of Alzheimer's disease showed that a clinical window can be achieved and selective ligands of the different mGluRs have been considered as useful tools to study neuroprotection.<sup>10–12</sup>

Structure–activity relationships of ligands interacting with NMDA receptors<sup>13</sup> show that an increase in the distance between the proximal and the distal acidic groups of Glu leads to NMDA antagonists. In general, the most potent NMDA antagonists bear a chain of four or six carbon atoms linking the two acidic groups, that is, (2*R*)-2-amino-5-phosphonopentanoic acid **2** [(2*R*)-AP5] and (2*R*)-2-amino-7-phosphonoheptanoic acid **3** [(2*R*)-AP7] (Fig. 1). It is noteworthy that the eutomer of the majority of NMDA ligands possesses an absolute configuration of the stereogenic center at the amino acidic moiety opposite to that of natural Glu, the endogenous neurotransmitter.

Homologation of the Glu backbone embedded in the selective ligands may lead to a significant modification of their pharmacological profile. For instance, the homo-derivative of (*S*)-AMPA **4** [(*S*)-Homo-AMPA] (Fig. 1) behaves as a selective agonist at mGluR6 (mGluRIII subtype) and completely loses the activity at AMPA receptors, which characterizes the reference compound.<sup>14</sup>

\* Corresponding author. Tel.: +39 02 5031 7516; fax: +39 02 5031 7565; e-mail: [gabriella.bombieri@unimi.it](mailto:gabriella.bombieri@unimi.it)

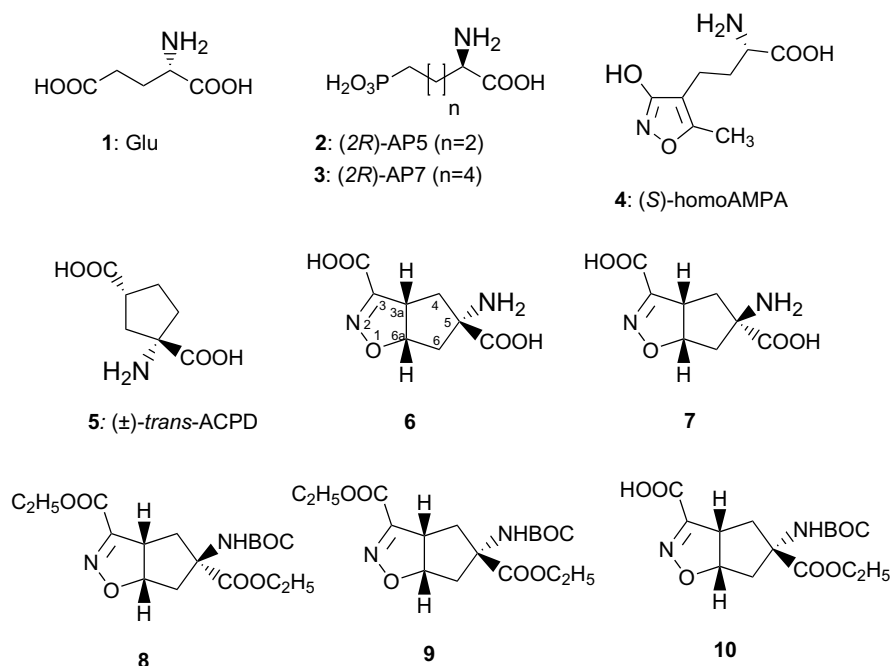


Figure 1. Chemical schemes.

Conformational studies on NMDA antagonists and mGluRs ligands, considering also amino acids constrained into the cyclic structures, showed that the majority of NMDA antagonists adopt a folded conformation with the proximal and the distal acidic functionalities oriented toward the same face of the molecule.<sup>13,15</sup> In contrast, Glu binds to the different types of mGluRs in a fully extended conformation, as in (±)-trans-ACPD **5** (Fig. 1). The selectivity between the mGluR subtypes can be achieved through the introduction of specific functionalities able to establish the additional interactions between the amino acids of the binding site.<sup>16,17</sup> In order to investigate further the conformational requirements needed for the selective interaction with NMDA and mGluRs, we have designed novel homologues of Glu, that is, 5-amino-4,5,6,6a-tetrahydro-3aH-cyclopenta[*d*]isoxazole-3,5-dicarboxylic acids (±)-**6** and (±)-**7**, characterized by an extended conformation locked in a bicyclic structure.<sup>18</sup> From the results of the pharmacological investigation, carried out by means of receptor binding techniques, second messenger assays and electrophysiological studies, amino acid (±)-**7** emerged as a very potent NMDA receptor antagonist supported by antagonist activity at mGluR1,5 (group I) and agonist activity at mGluR2.<sup>18</sup>

The two diastereoisomers (+)-**6**, (–)-**6** and (+)-**7**, (–)-**7** were subsequently prepared and the absolute configuration was assigned by vibrational circular dichroism analyses.<sup>19</sup> The single stereoisomers were submitted to the biological assays. Quite interestingly, the mixed activity at mGluRs and receptors of racemate (±)-**7** turned out to be the overlap of the NMDA antagonist activity of its enantiomer (+)-**7** with the mGluR activity of enantiomer (–)-**7**.<sup>20</sup> The pharmacological profile of amino acid

(±)-**7** candidates it as a new lead for neuroprotective agents. This hypothesis was confirmed by an in vitro model of cerebral ischemia based on cultured murine cortical cells exposed to oxygen and glucose deprivation (OGD); derivative (±)-**7** produced a marked neuroprotective activity. Interestingly, the effect was particularly evident with enantiomer (+)-**7**, which is provided with NMDA receptor antagonist activity.<sup>20</sup> The above-reported results could be employed in the design of new ligands in case we possess sound information on the conformational profile of the tested ligands and reliable receptor models. For such a purpose, we were interested to know the conformation in the solid state of amino acids **6** and **7**. Since we were unable to obtain crystals suitable for X-ray diffraction analyses, we performed our investigation on their precursors **8**, **9**, and **10**. Herein, we report their crystal structures and a discussion of the results.

## 2. Results and discussion

### 2.1. Crystal structures description

Compound **8** represents the (3a*S*,5*R*,6a*S*)-epimer of 5-*tert*-butoxycarbonylamino-4,5,6,6a-tetrahydro-3aH-cyclopenta[*d*]isoxazole-3,5-dicarboxylic acid diethyl ester. An ORTEP<sup>21</sup> view of the molecule is shown in Figure 2.

The cyclopentane moiety with puckering parameters<sup>22</sup>  $Q = 0.421(1)$  Å and  $\varphi_2 = 67.2(1)^\circ$  has an envelope conformation with the C(3) atom (arbitrary numbering) out of the plane of the remaining ring atoms by  $-0.644(9)$  Å.

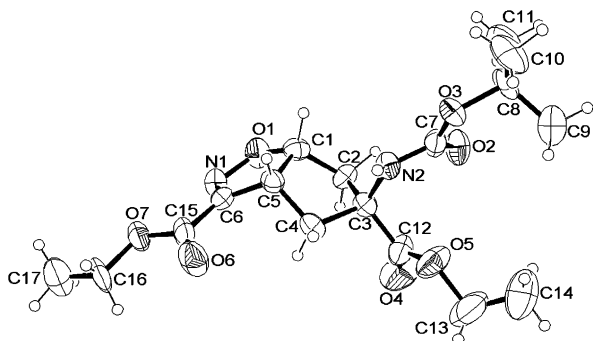


**Figure 2.** ORTEP view of compound **8**, showing the atom-numbering scheme (ellipsoids are at the 50% probability and H atoms are as spheres of arbitrary radii).

The BOC moiety at C(3) occupies a pseudo axial position, characterized by a torsion angle C(5)–C(4)–C(3)–N(2) of 76.2(8)°. The ethyl ester chain has a pseudo equatorial orientation with a torsion angle C(1)–C(2)–C(3)–C(12) of 158.6(8)°. The dihedral angle between the two rings is 117.9(3)°.

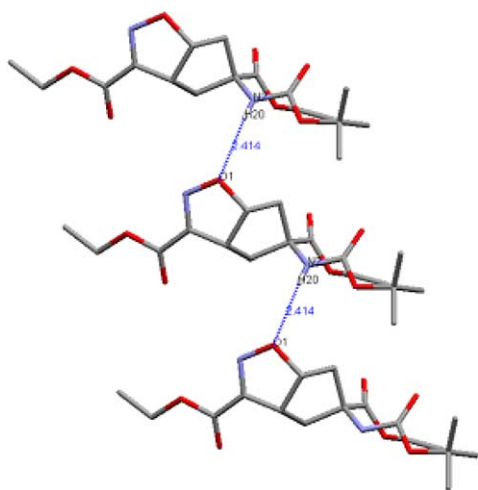


**Figure 3.** Chain formation in compound **8** via intermolecular hydrogen bonds along the *a*-axis.

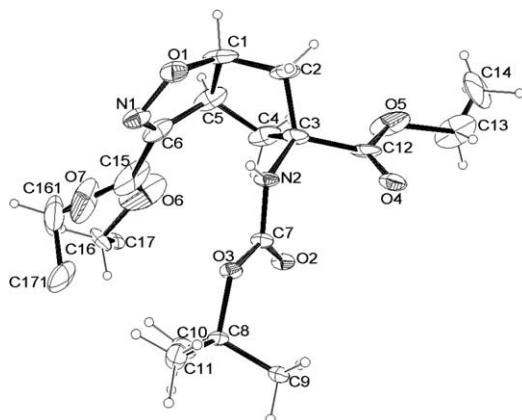
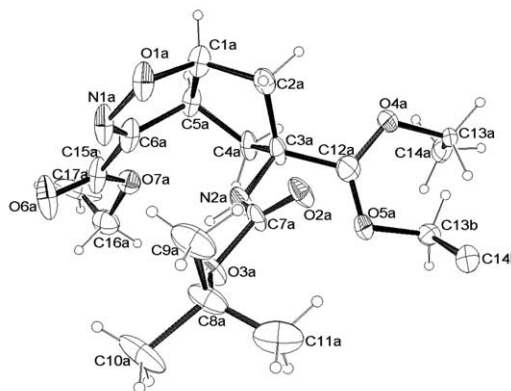


**Figure 4.** ORTEP view of the asymmetric unit of compound **9**, showing the atom-numbering scheme (ellipsoids are at 30% probability and H atoms are as spheres of arbitrary radii).

The N(2) proton is involved in an intermolecular hydrogen bond interaction characterized by the distances N2···O1' of 3.11(1) Å and H(20)···O(1)' of 2.41(7) Å, angle N(2)–H(20)–O(1) of 175(8)° (' at  $x+1, y, z$ ), as shown in Figure 3, which leads to the formation of independent molecular chains in the *a*-axis direction.

Compound **9** (3*aS*,5*S*,6*aS*)-5-*tert*-butoxycarbonylamino-4,5,6,6*a*-tetrahydro-3*aH*-cyclopenta[*d*]isoxazole-3,5-dicarboxylic acid diethyl ester, that is, epimer **8**, has been already investigated at room temperature,<sup>18</sup> but the presence of highly disordered terminal groups (the ethyl chains) suggested a re-examination of the crystal structure at low temperature (100 K). The new structure refinement did not give a significant improvement in the disorder that remains also at low temperature. However, significant observations not described previously can be made concerning the structural differences in the two independent molecules of **9** forming the asymmetric unit (see Fig. 4). What is noticeable is the presence of intermolecular interactions N(2)···O(5A)', with distances 3.04(1) Å and H(20)···O(5A)' of 2.27(1) Å, angle 148.0(4)° and O(4)···N(2A)' 2.95(1) Å, H(20A)···O(4)' 2.16(1) Å, angle 152.8(5)° (' at  $\frac{1}{2}-x, 1-y, \frac{1}{2}+z$ ) in both molecules; significant hydrogen bond interactions, which determine dimer formation are depicted in Figure 5.

The two molecules differ in the position of the BOC moiety that determines, in the not A labeled, an orientation of the BOC nitrogen hydrogen in the direction of the isoxazole oxygen O(1) with a distance of N(2)···O(1) of 3.06(1) Å. The value N(2)–H(20)···O(1) of 2.65(1) Å, with an angle N(2)–H(20)–O(1) of 140.4(5)°, is not suitable for a hydrogen bond, could be significant as it represents a possible transition state for the formation of **9**. In the second molecule (A labeled), the BOC moiety presents an opposite orientation of the nitrogen hydrogen, with a distance N(2A)–H(20A)···O(1A) of 3.16(1) Å and the torsion angle C(2A)–C(3A)–N(2A)–H(20A) of 111.4(8)°. This means, at least in the solid state, that only the first orientation of BOC can explain the transition state in the formation of **9**. The dihedral angle between the two pentatomic rings does not change



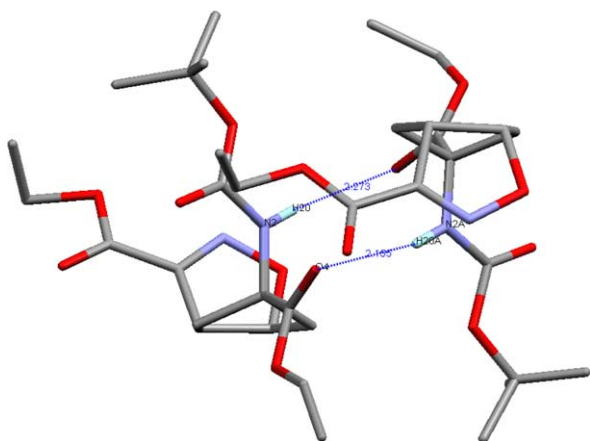


**Figure 5.** Particular of the dimer formation (the H bond distances are reported).

from **8**, being  $119.1(4)^\circ$  [ $118.3(4)^\circ$  for the A labeled molecule], while the puckering parameter  $Q^{22}$  of the cyclopentane ring is lowered, with respect to compound **8**, at  $0.386(9) \text{ \AA}$  [ $0.313(9) \text{ \AA}$  for the A labeled] and  $\varphi_2 = 71.1(9)^\circ$  [ $\varphi_2 = 69.5(7)^\circ$ ], characteristic in both for an envelope conformation, with C(3) out of the ring plane of  $-0.592(7)$  and  $0.560(7) \text{ \AA}$ , respectively.

For the subsequent hydrolysis of one of the ethyl ester moiety of ( $\pm$ )-**9**, compound ( $\pm$ )-**10** was obtained (Fig. 6).

In this case, the ethyl chain is no longer disordered in the solid state and the overall molecular conformation is close to that of **9**, with the BOC position 'mid-way' between the two observed in compound **9**, as shown in Figure 7.

The dihedral angle between the two pentatomic rings is  $119.7(2)^\circ$  and the puckering parameters<sup>22</sup>  $Q = 0.344(5) \text{ \AA}$ , while  $\varphi_2 = 77.3(7)^\circ$  of the cyclopentane does not differ significantly with respect to **9** and the C(3) is out of the ring plane of  $-0.537(4) \text{ \AA}$ . The N(2) hydrogen and

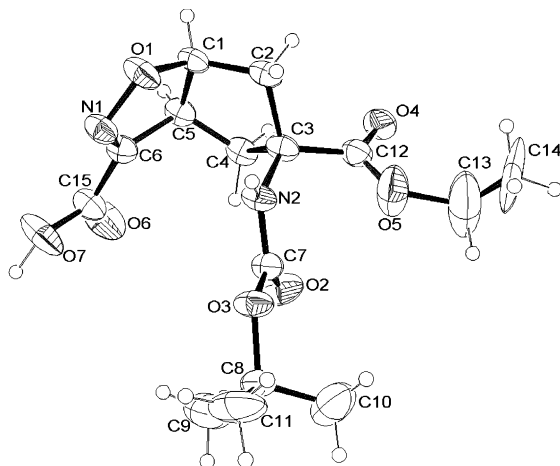


**Figure 6.** ORTEP view of racemic compound **10**, showing the atom-numbering scheme (ellipsoids are at 50% probability and H atoms are as spheres of arbitrary radii).

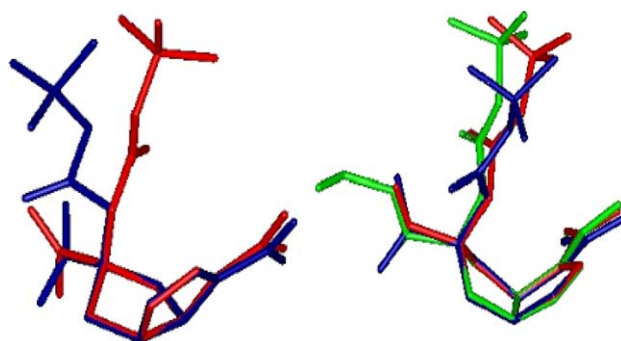


**Figure 7.** Left: superimposition of the two independent molecules of **9** (A labeled in blue); the disordered chains are omitted for the sake of clarity. Right: the two molecules are compared with the corresponding acid **10** in green.

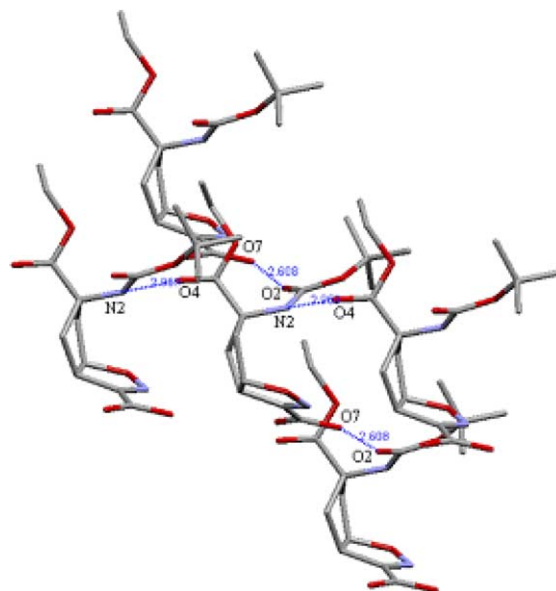


**Figure 8.** Intermolecular hydrogen bonds scheme view along the  $b$ -axis (the donor-acceptor distances are reported) for compound **10**.

the proton of the acid moiety are in this case involved in the intermolecular interactions with adjacent molecules allowing for the formation of a three-dimensional network of hydrogen bonds: N2–H21'...O4' at a distance of  $2.11(5) \text{ \AA}$ , angle  $173(4)^\circ$  (' at  $x, -y, z + \frac{1}{2}$ ), O7–H7...O2'' at a distance of  $1.61(8) \text{ \AA}$ , angle  $178(7)^\circ$  (' at  $x + \frac{1}{2}, y - \frac{1}{2}, z + \frac{1}{2}$ ), as reported in Figure 8.

The conformational mobility around the single bonds C(3)–C(12) and C(6)–C(15) between the bicyclic ring and the carboxylate groups has been compared with the results obtained by a relaxed potential energy scan (PES)<sup>19</sup> on the torsion angles N(2)–C(3)–C(12)–O(5) and N(1)–C(6)–C(15)–O(7), which showed two potential energy minima at  $2^\circ$  and  $182^\circ$  for the first (connecting the 4,5 dihydroisoxazole ring to the carboxylate group) and  $128^\circ$  and  $308^\circ$  for the second (connecting the cyclopentane to the carboxylate group). The X-ray data show that the two possible rotations around C(3)–C(12) are



present in the examined compounds with the values being  $31(1)^\circ$  in **8**,  $34(1)^\circ$ , and  $166(1)^\circ$  for the two molecules of **9** and  $12(1)^\circ$  in **10**, while for that concerning the rotation around C(6)–C(15) no correlation exists with the crystallographic results being  $-13(1)^\circ$  for **8**,  $-178(1)^\circ$ , and  $7(1)^\circ$  for **9**, and  $4(1)^\circ$  for **10**. In respect to this, it is interesting to note that the N(1)–C(6)–C(15)–O(7) moiety, at least in the solid state, is not heavily involved in intermolecular interactions and this gives more flexibility to the group. Compound **8** is the precursor of **7** that displays a noticeable antagonism at NMDA receptor ( $K_i = 0.37 \mu\text{M}$ ),<sup>18</sup> on the basis of the proposed bioactive conformation of CIP-A,<sup>23</sup> whose pharmacophoric pattern is represented by three ionizable centers  $\text{N}^+$ , C- $\alpha$ , and C- $\omega$  at the distances  $d_1$  ( $d_{\text{N},\text{C}-\omega}^+$ ) 4.18 Å and  $d_2$  ( $d_{\text{C}-\alpha,\text{C}-\omega}$ ) 4.43 Å. In the studied compounds **8**, **9**, and **10**,  $\text{N}^+$ , C- $\alpha$ , and C- $\omega$  correspond to bicyclic components, where C- $\alpha$  bears an ester chain and C- $\omega$  is the C(3) carbon. In **8**,  $d_1$  is 4.16 Å in agreement to 4.18 Å, while 3.63 Å is significantly shorter than  $d_2$  CIP-A, thus giving a reason for its lower activity. It is interesting to note that compound **8** gives  $d_1$  and  $d_2$  distances also shorter with respect to that proposed for the Hutchison's pharmacophoric model<sup>15</sup> of NMDA antagonists, which gave  $d_{\text{N},\text{C}-\omega}^+$  5.55 Å and  $d_{\text{C}-\alpha,\text{C}-\omega}$  5.54 Å as optimal values, contributing to explain the lower potency of the derived compound **7** with respect to the potent antagonist CGS19755 ( $K_i = 0.095 \mu\text{M}$ ),<sup>13</sup> which better match the Hutchison model. Its stereoisomer **9** and the derived acid **10** have, as expected on geometrical grounds, comparable values for  $d_1$  and  $d_2$  being 3.54 and 3.20 Å in **9** (averaged values of the two independent molecules) and 3.63 and 3.23 Å in **10**, that can be related to the inactivity of **6** for NMDA receptor.

### 3. Conclusion

The reported crystallographic analysis established the molecular conformation of three key intermediates toward the synthesis of novel bicyclic amino acids, acting at the glutamate receptors. In **8**, the C(3) stereochemical conformation determines the N(2) proton orientation favorable for the hydrogen bond formation with the isoxazole O(1) of an adjacent molecule. In epimer **9**, the change of configuration at C(3) allows dimer formation with the involvement of an ester sequence bound to C(3). When one of the ethyl ester moieties of **9** is hydrolyzed, the stereochemical configuration is retained and the hydrogen bond characteristic of **9** is still present with an additional hydrogen bond between the O(7) proton of the acid moiety and the O(2) of the BOC group.

The analysis of the distances between the Hutchinson model charged atoms for the pharmacophore responsible for bioactivity shows that in the precursor **8** they provide reason for the NMDA antagonism of the derived product; this was not verified for **9** and **10** as they do not match the pharmacophore request and their products in fact are not NMDA antagonists.

However, the crystal structures of these molecules provide detailed insight into the three-dimensional conformation of this class of compounds, useful for understanding their behavior at a molecular level, as docking studies are currently in progress. This atomic resolution knowledge could be helpful for assessing the relationship between the structure–activity relationships and could be employed to develop new subtype-selective ligands.

**Table 1.** Crystal and structure refinement for compounds **8**, **9**, and **10**

Compound	<b>8</b>	<b>9</b>	<b>10</b>
Empirical formula	$\text{C}_{17}\text{H}_{26}\text{N}_2\text{O}_7$	$\text{C}_{17}\text{H}_{26}\text{N}_2\text{O}_7$	$\text{C}_{15}\text{H}_{22}\text{N}_2\text{O}_7$
Formula weight	370.40	370.40	342.35
Crystal system	Orthorhombic	Orthorhombic	Monoclinic
Space group	$P2_12_12_1$	$P2_12_12_1$	$Cc$
Unit cell. dim. (Å, °)	$a = 6.186(5)$ $b = 17.292(9)$ $c = 18.199(9)$	$a = 10.538(5)$ $b = 18.053(5)$ $c = 19.937(5)$	$a = 10.514(4)$ $b = 16.923(4)$ $c = 10.376(2)$ $\beta = 108.56$
Temperature (K)	293	100	293
Volume (Å <sup>3</sup> )	1938.8(1)	3793(9)	1750.2(7)
Z	4	8	4
Calc. Dens. (Mg/m <sup>3</sup> )	1.269	1.236	1.299
Abs. Coeff. (mm <sup>-1</sup> )	0.099	0.101	0.104
$F(000)$	792	1584	728
Crystal size (mm)	$0.06 \times 0.07 \times 0.10$	$0.11 \times 0.16 \times 0.09$	$0.09 \times 0.12 \times 0.08$
$\theta$ Range (°)	1.50–24.99	1.50–21.26	2.37–24.98
Limiting indices	$-7 \leq h \leq 7$ $-1 \leq k \leq 20$ $-1 \leq l \leq 21$	$-10 \leq h \leq -10$ $-18 \leq k \leq 18$ $-20 \leq l \leq 20$	$-12 \leq h \leq 12$ $-20 \leq k \leq 20$ $-1 \leq l \leq 12$
Refl. Coll./unique	3201/2599	22849/4225	3584/1825
Refinement method		Full-matrix least-squares on $F^2$	
Goodness-of fit	0.979	1.048	1.021
Final $R$ ( $F^2$ )	$R1 = 0.0586$	$R1 = 0.0833$	$R1 = 0.0449$
$[I > 2\sigma(I)]$	$wR2 = 0.1294$	$wR2 = 0.1837$	$wR2 = 0.1015$

#### 4. Experimental

Crystals of **8** and **9** were obtained from ethyl acetate and **10** from an ethanolic solution at room temperature as colorless platelets. An Enraf Nonius CAD-4 diffractometer was used for data collection (compounds **8** and **10**) at room temperature (MoK $\alpha$  radiation,  $\lambda$  0.71073), while for **9** low temperature data (100 K) were collected on a Bruker-Axs SMART-CCD detector diffractometer (MoK $\alpha$  radiation). The lattice parameters were determined by least-squares refinements of 25 high angle reflections. The structures were solved by direct methods (Sir92<sup>24</sup>) and the refinements carried out by full-matrix least-squares. All non-H-atoms were refined anisotropically. The H-atoms positions were detected in a difference Fourier synthesis and refined with isotropic thermal factors, or introduced in calculated positions in their described geometries and allowed to ride on the attached carbon atom with fixed isotropic thermal parameters (1.2U<sub>eq</sub> (C) for CH/CH<sub>2</sub> and 1.5U<sub>eq</sub> (C) for CH<sub>3</sub>). Refinements were carried out with SHELX-97.<sup>25</sup> In the absence of any significant anomalous scatterer for MoK $\alpha$  radiation, the absolute configuration of **8** and **9** was not determined from diffraction studies but assigned by vibrational circular dichroism spectra.<sup>19</sup> A summary of the crystal data, data collection, and structure refinement is presented in Table 1. CCDC numbers [275412 (**8**), 275410 (**9**), and 275411 (**10**)] contain the supplementary crystallographic data for this paper. These data can be obtained free of charge via [www.ccdc.cam.ac.uk/conts/retrieving.html](http://www.ccdc.cam.ac.uk/conts/retrieving.html) (or from the Cambridge Crystallographic Data Centre, 12, Union Road, Cambridge CB2 1EZ, UK; fax: (+44)1223-336-033; or deposit@ccdc.cam.ac.uk).

#### Acknowledgments

This work was financially supported by MIUR-CO-FIN2003 and by the University of Milano (FIRST).

#### References

1. *Excitatory Amino Acids and Synaptic Transmissions*; Wheal, H. V., Thomson, A. M., Eds.; Academic Press: London, 1995.
2. Bräuner-Osborne, H.; Egebjerg, J.; Nielsen, E. Ø.; Madsen, U.; Krosgaard-Larsen, P. *J. Med. Chem.* **2000**, *43*, 2609.
3. Ozawa, S.; Kamiya, H.; Tsuzuki, K. *Prog. Neurobiol.* **1998**, *54*, 581.
4. *The Ionotropic Glutamate Receptors*; Monaghan, D. T., Wenthold, R. J., Eds.; Humana Press: Totowa, NJ, 1997.
5. *Handbook of Experimental Pharmacology, Ionotropic Glutamate Receptors in the CNS*; Jonas, P., Monyer, H., Eds.; Springer: Berlin, 1999; Vol. 141.
6. Conn, P. J.; Pin, J. P. *Ann. Rev. Pharmacol. Toxicol.* **1997**, *37*, 205.
7. Arias, R. L.; Tasse, J. R. P.; Bowlby, M. R. *Brain Res.* **1999**, *816*, 299.
8. Palmer, G. C. *Curr. Drug Targets* **1991**, *2*, 241.
9. Herling, P. L. *Excitatory Amino Acids—Clinical Results with Antagonists*; Academic Press: London, 1997.
10. Pellicciari, R.; Costantino, G. *Curr. Opin. Chem. Biol.* **1999**, *3*, 433.
11. Monn, J. A.; Valli, M. J.; Massey, S. M.; Wright, R. A.; Salhoff, C. R.; Johnson, B. G.; Howe, T.; Alt, C. A.; Rhodes, G. A.; Robey, R. L.; Griffey, K. R.; Tizzano, J. P.; Kallman, M. J.; Helton, D. R.; Schoepp, D. D. *J. Med. Chem.* **1997**, *40*, 528.
12. Weiser, T. *Curr. Pharm. Design* **2002**, *8*, 941.
13. Johnson, G.; Ornstein, P. L. *Curr. Pharm. Design* **1996**, *2*, 331.
14. Ahmadian, H.; Nielsen, B.; Bräuner-Osborne, H.; Johansen, T. N.; Stensbøl, T. B.; Sløk, F. A.; Sekiyama, N.; Nakanishi, S.; Krosgaard-Larsen, P.; Madsen, U. *J. Med. Chem.* **1997**, *40*, 3700.
15. Hutchison, A. J.; Williams, M.; Angst, C.; De Jesus, R.; Blanchard, L.; Jackson, R. H.; Wilusz, E. J.; Murphy, D. E.; Bernard, P. S.; Schneider, J.; Campbell, T.; Guida, W.; Sills, M. A. *J. Med. Chem.* **1989**, *32*, 2171.
16. Kozikowski, A. P.; Steensma, D.; Araldi, G. L.; Tückmantel, W.; Wang, S.; Pshenichkin, S.; Surina, E.; Wroblewski, J. T. *J. Med. Chem.* **1998**, *41*, 1641.
17. Jullian, N.; Brabet, I.; Pin, J. P.; Acher, F. C. *J. Med. Chem.* **1999**, *42*, 1546.
18. Conti, P.; De Amici, M.; Joppolo di Ventimiglia, S.; Stensbøl, T. B.; Madsen, U.; Bräuner-Osborne, H.; Russo, E.; De Sarro, G.; Bruno, G.; De Micheli, C. *J. Med. Chem.* **2003**, *46*, 3102.
19. Roda, G.; Conti, P.; De Amici, M.; He, J.; Polavarapu, P. L.; De Micheli, C. *Tetrahedron: Asymmetry* **2004**, *15*, 3079.
20. Conti, P.; De Amici, M.; Grazioso, G.; Roda, G.; Pinto, A.; Bø Hansen, K.; Nielsen, B.; Madsen, U.; Bräuner-Osborne, H.; Egebjerg, J.; Vestri, V.; Pellegrini-Giampietro, D. E.; Sibille, P.; Acher, F. C.; De Micheli, C. *J. Med. Chem.*, submitted for publication.
21. Farrugia, L. J. ORTEP-3 for Windows a version of ORTEP-III with graphical user interface (GUI). *J. Appl. Cryst.* **1997**, *30*, 565.
22. Cremer, D.; Pople, J. A. *J. Am. Chem. Soc.* **1975**, *97*, 1354.
23. Conti, P.; De Amici, M.; De Sarro, G.; Rizzo, M.; Stensbøl, T. B.; Bräuner-Osborne, H.; Madsen, U.; Toma, L.; De Micheli, C. *J. Med. Chem.* **1999**, *42*, 4099.
24. SIR-92: Altomare, A.; Burla, M. C.; Camalli, M.; Cascarano, G.; Giacovazzo, C.; Gagliardi, A.; Polidori, G. *J. Appl. Crystallogr.* **1994**, *27*, 435.
25. Sheldrick, G. M. SHELXL97, Program for refinement of crystal structure. University of Göttingen, Germany, 1997.